Bidirectional interleaved dc-dc converter for supercapacitor–based energy storage systems applied to microgrids and electric vehicles

R. R. Melo, F. L. M. Antunes, and S. Daher
FEDERAL UNIVERSITY OF CEARÁ
Campus do Pici – Caixa Postal 6001 – CEP 60455-760
Fortaleza, Brazil
Tel.: +55 / (85) 3366 9580
Fax: +55 / (85) 3366 9574
E-Mails: rodnei.melo@ifce.edu.br, fantunes@dee.ufc.br, sdaher@dee.ufc.br
URL: http://www.gpec.ufc.br

Keywords

«Interleaved converters», «Supercapacitors», «Microgrids», «Electric Vehicles».

Abstract

This paper presents a survey on supercapacitors and their application as power supply in microgrids (MGs) and electric vehicles (EVs). The importance of efficient dc-dc converters in this case is also discussed. One of the main topologies adequate for this purpose is discussed in detail i.e. the bidirectional interleaved boost converter. Finally, the design of a 2-kW prototype is presented so that a 165-F/48-V supercapacitor module can be connected to a 96-V dc link. Simulation and experimental results are also presented to validate the theoretical assumptions.

Introduction

Capacitors are devices that have been commercially available for decades, which are used to store small amounts of energy and able to be charged and discharged hundreds of thousands times. Nanotechnology has enabled the emergence of capacitors that store hundreds of times more energy per unit volume or weight than their traditional counterparts. This new generation of devices is called supercapacitors, while it represents high-power energy storage elements if compared with conventional capacitors. Supercapacitors are so-called because their respective capacitances are of the order of thousands of farads, which are virtually impossible in conventional capacitors [1].

The use of such technology has been increasingly explored associated with power electronics, thus improving the performance MGs and EVs [1], [15], [21], [24], [26]. In such systems, supercapacitors (SCs) have become critical in the maintenance of the voltage balance across the dc links. Within this context, this work presents the evaluation of some dc-dc converter topologies and also the design of a bidirectional dc-dc converter rated at 2 kW to connect a 165-F/48-V supercapacitor module to a 96-V dc link to supply EVs. The chosen topology is the bidirectional interleaved boost converter. A laboratory prototype is also implemented and evaluated through simulation and experimental tests.

Supercapacitors

In recent years, SCs have presented some major improvements. They are characterized by the very low equivalent series resistance (ESR), thus allowing them to provide high currents and store large amounts of charge in a short period. By using high technology in the manufacturing process, it is possible to obtain a solid-state energy storage system based on carbon nanotubes which is perfectly rechargeable. Besides, nanoscale provides a large surface area for the accumulation of electrons and the exceptional increase in capacitance [13], [18]. SCs or electrical double-layer capacitors (EDLCs) are components able to store hundreds of times more energy than a standard capacitor or even a battery, while maintaining the ability to be charged and discharged faster [10], [13], [20], [24].

Energy storage in a conventional capacitor occurs in the dielectric material between its plates, which can be polarized on the application of an electric field. As the internal dipoles are aligned within the dielectric, an electric field is established. The capacitance increases proportionally with the plate area, while the stored energy can be calculated according to the following expression [13], [18]:

$$E = \frac{1}{2} \cdot C \cdot V^2 \quad (1)$$

where C is the capacitance in farads and V is the voltage measured in volts.

Supercapacitors achieve the same result, but by mass separation and movement of charges. The mechanism for moving opposite charges to different sides of a separator is very similar to electrochemistry and battery technology, although it is not a chemical reaction. Fig. 1 shows the schematic representation of a supercapacitor [10]. Basically, the supercapacitor can be represented by a simple RC circuit. How fast the stored energy can be discharged depends on the internal resistance of the device. The development of new materials has allowed the conception of SCs with reduced ESR, which are ideal for fast discharge applications [18].

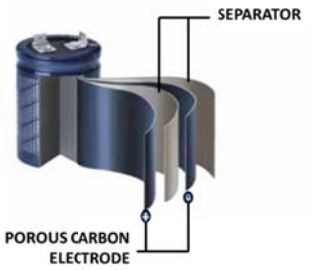

Fig. 1: Structure of a SC [10]

Table 1 presents a comparison involving some energy storage elements [13], [20].

Table I: Comparison among energy storage elements

Performance Characteristics	Battery	Conventional Capacitor	Supercapacitor
Charging time	1 to5 hours	10^{-6} to 10^{-3} s	0.3 to 30 s
Discharge time	0.3 to 3 hours	10^{-6} to 10^{-3} s	0.3 to 30 s
Energy (Wh/kg)	10 to 100	<0.1	1 to 10
Life cycle	1,000	>500,000	>500,000
Specific power (W/kg)	<1,000	<100,000	<10,000
Efficiency during charging/discharging	0.7 to 0.85	>0.95	0.85 to 0.98

Supercapacitors have low power density if compared with batteries, but there are some remarkable advantages for applications involving hybrid [1], [10], [12], [13], [20], [25]:

- Fast charge and discharge (seconds);
- Long life: EDLCs (2.5 V, 2.7 V, and 3V) – >500,000 cycles;
- High power density (10 times greater than a battery);
- High efficiency (higher than 95%);
- Wide operating temperature range (-25 °C/ 70 °C);
- Environmentally correct.

Supercapacitors have been increasingly used in numerous applications, as much as its dielectric-based counterparts. There are basically two manufacturers responsible for the commercial availability of supercapacitors in terms of cells and modules. Fig. 2(a) shows some commercial modules rated at 48 V and 166 F and manufactured by NessCap [20]. On the other hand, Fig.2 (b) and Fig.2 (c) represent two modules rated at 48 V/165 F [12] and 48.6 V/165 F [10], which are manufactured by Maxwell and LSMtron, respectively.



(a) EMHSR-0166C0-048R0S (b) BMOD0165 P048 BXX (c) LSUM 050R4P 0166F EA

Fig. 2: Supercapacitor modules

New versions of circuit simulation software typically present a supercapacitor model in the component libraries. For instance, Matlab version R2013b [11] presents a generic model of the supercapacitor, where the parameters can be properly adjusted. After that, it is possible to plot three graphs to analyze the behavior of the supercapacitor. Fig. 3 shows some curves regarding a supercapacitor module rated at 165 F and 48 V, which can be obtained in Matlab R2013b. It is worth to mention that the charge current is fixed at 20 A.

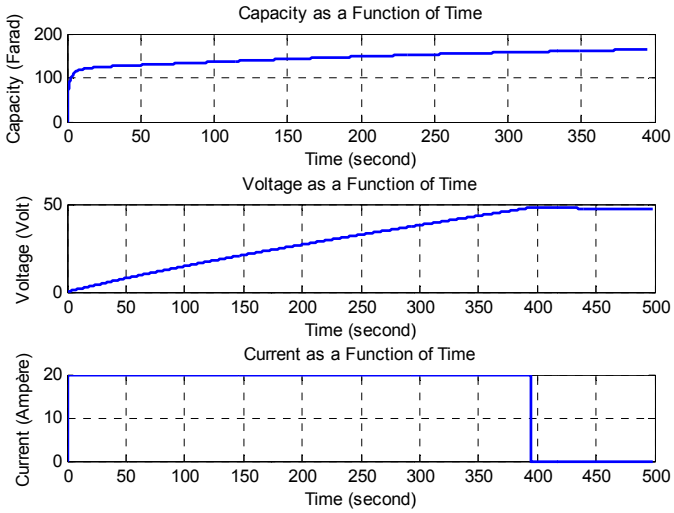

Fig. 3: Curves obtained by simulation for a 165-F/48-V supercapacitor: (a) Capacitance versus time (b) Voltage versus time (c) Current versus time

During the supercapacitor charge, the following expression is valid:

$$I = C \cdot \frac{dv}{dt} \rightarrow \frac{I}{C} = \frac{dv}{dt} \tag{2}$$

Considering that the aforementioned supercapacitor module is charged by a constant current source of 20 A, the charge time can be determined by dividing the rated voltage of the module by ratio given by expression (2) as:

$$\frac{I}{C} = \frac{20}{165} = 121.21\ mV/s \rightarrow \frac{48}{0.12121} = 396\ s = 6.6\ min \tag{3}$$

The obtained result is analogous to that provided by software Matlab. The manufacturer Maxwell Technologies mentions that charge or discharge time are nearly the same because the energy storage process of the supercapacitor is not a chemical reaction.

DC-DC Converter

For the application of supercapacitors as a source for fast energy transfer in either MGs or EVs, power flow must be controlled by a proper device. Thus it is possible to step the voltage across SCs up or down according to a given application. For this purpose, dc-dc converters (also known as choppers) can be designed to control the energy transfer from a nonregulated dc input voltage source to the load, which must be supplied by a regulated dc voltage. Choppers are usually employed as switch-mode power supplies (SMPSs) and are able to drive an active switch represented by a BJT (Bipolar Junction Transistor), a MOSFET (Metal Oxide Semiconductor Field Effect Transistor), or an IGBT (Insulated Gate Bipolar Transistor) by using PWM (Pulse Width Modulation) with fixed frequency [4], [19], [22], [23]. Fig. 4 represents the application of supercapacitors to MGs and EVs.

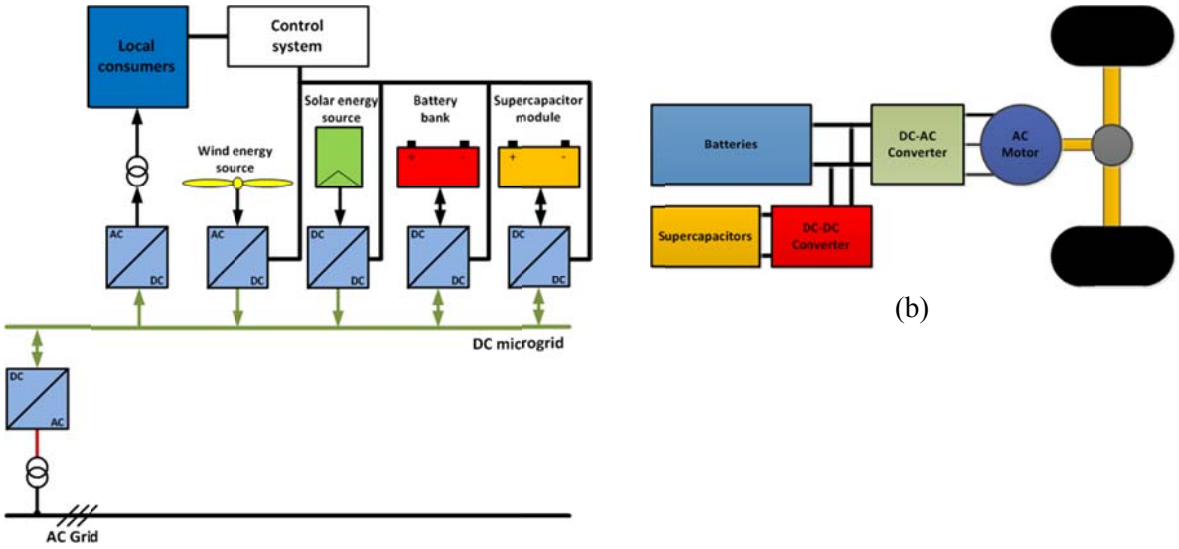

(a)

Fig. 4: (a) Microgrid, (b) Electric Vehicle

The use of dc-dc converters associated with the supercapacitors has been the scope of several works in literature that aim at an optimum cost-benefit ratio and also good performance. One of the most popular topologies is the bidirectional interleaved dc-dc converter. By using the interleaving technique, the converter becomes adequate in the achievement of high power levels, while significant advantages in terms of reduced current ripple and power sharing among the interleaved cells are achieved [3], [6], [8], [9], [17]. However, this type of structure requires attention on the voltage balancing and isolation of faulty cells.

Bidirectional Interleaved Boost Converter

Within this context, a practical approach for SC applications is proposed in this paper, which consists in using the bidirectional interleaved boost converter shown in Fig. 5. Two sawtooth waves phase-displaced by 180° are used to obtain the drive signals for the active switches. Besides, the switches in a given leg operate in a complementary way. It is also worth to mention that two, three, or four legs can be typically used depending on the power level [3], [4], [9].

The converter is supplied by a SC module (V_1) and connected a dc link (V_2). The converter operates in boost mode when energy is transferred from the SC module to the dc link. On the other hand, operation in buck mode occurs when energy is transferred from the dc link to the SC module. In this case, operation is supposed to maintain the stability of the dc link.

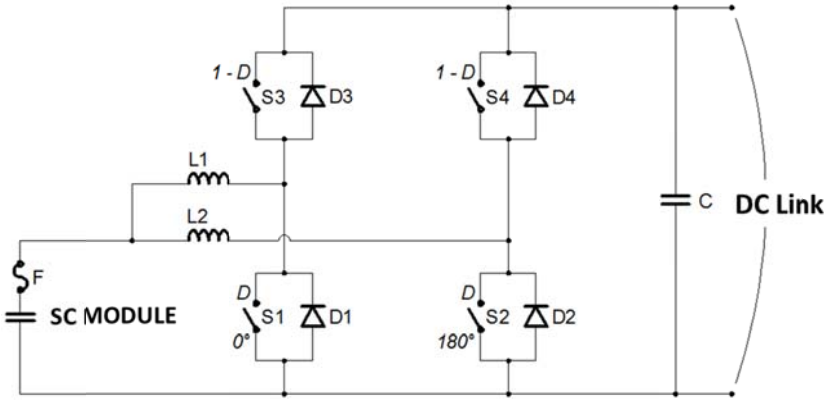

Fig. 5: Proposed bidirectional interleaved dc-dc converter

The reduction of the current ripple is proportional to the increase in the number of cells of phases represented by *n* in the interleaved converter. Thus the switching period for a given leg is less than *n* times the switching period of a conventional boost converter [3], [4], [9], [17]. In order to process the total amount of energy flowing through the system, the discharge voltage across the supercapacitor modules must not be less than 50% of the maximum voltage [2], [6].

Design of the proposed converter

According to the qualitative and quantitative analysis of the converter, it is possible to define the design procedure that allows the implementation of an experimental prototype. The operation of the converter in buck and boost modes is symmetrical, since both them are complementary in terms of the duty cycles applied to the active switches [8], [9], [19]. Therefore it is only necessary to analyze one of the aforementioned modes to define the design procedure.
The ripple current through in the inductors (L_1 and L_2) is a function of the maximum input current. As it was mentioned before, the converter phases are displaced by 180°, this leading to the partial cancellation of the input current ripple. It is also important to define the maximum stress for the supercapacitor module during the discharging process considering the maximum input current. Therefore, the specifications of the converter prototype are given as follows:

P_2=2 kW	Rated output power;
V_1=48 V	Rated voltage across the supercapacitor module;
V_2=96 V	Rated voltage across the dc link;
f_s=20 kHz	Switching frequency;
ΔV_2=2%V_2	Ripple voltage across the dc link;
ΔI_{L1}=ΔI_{L2}=10%I_1	Maximum ripple current through the inductors;
$V_{1(MIN)}$=0.5V_1	Maximum discharge voltage across the supercapacitor module;
η=96%	Efficiency of the converter.

Considering the technical characteristics of the supercapacitor module, which voltage should not be over V_1=48 V, the converter must operate with the duty cycle varying between 0.5 and 0.75. The components are designed considering such the aforementioned range and also the maximum input current, so maximum current stress has been considered. By using simulation software PSIM®, some important current and voltage waveforms can be obtained. The values obtained in the simulation tests are in accordance with the design procedure. Fig. 6 presents some waveforms for the condition where the voltage across the supercapacitor module is 24 V i.e. 50% of the rated voltage. According to the rated power, it is possible to calculate the input current and also the average current throught the inductors.

$$P1 = \frac{P2}{\eta} = \frac{2000}{0.96} = 2.083\ kW \rightarrow I1 = \frac{P1}{V1_{MIN}} = 86.8\ A \rightarrow IL1_{MED} = IL2_{MED} = \frac{I1}{2} = 43.4\ A \qquad (4)$$

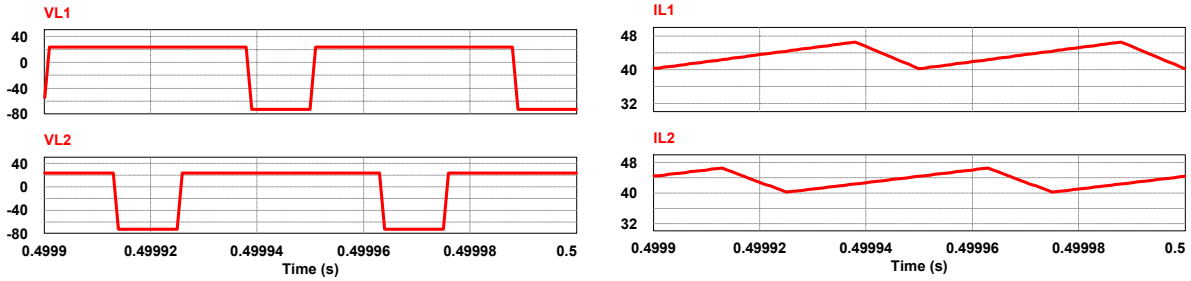

(a) Voltage across and current through inductors

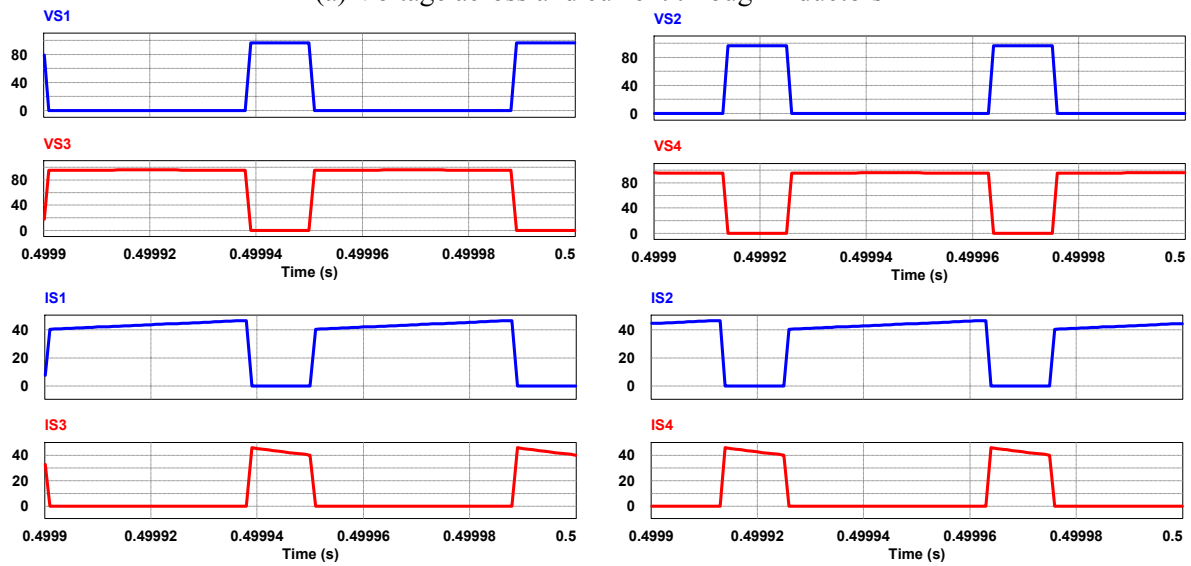

(b) Voltage across and current through the active switches

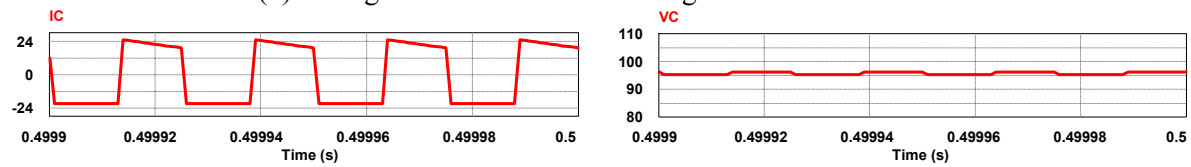

(c) Voltage across and current through the output capacitor

Fig. 6: Voltage and current waveforms representing the converter operation

From the current and voltage stresses regarding the converter elements obtained in both design procedure and simulation tests, it is possible to choose the components detailed in Table II for the prototype implementation. In order to increase efficiency and reduce losses in magnetic components, the inductors were implemented using toroidal cores manufactured by Iron Power.

Table II: Components used in the prototype

Components	Specification	Model	Quantity
Switches	MOSFETs rated at 171 A/150 V	IRFP4568PbF - International Rectifier	4
Inductors	310 µH	Toroidal core T300-52D - Micrometals	2
Capacitors	680 µF/150 V	B43505 - Epcos	7

The drive circuit of the active switches and the control system have been designed so that the voltage across the dc link remains constant at V_2=96 V. For this purpose, it is first necessary to obtain the small signal model of the converter so that the relevant transfer functions can be obtained. In order to properly design the control loops, the n-phase bidirectional interleaved boost converter can be simplified in the form of a one-phase topology. By using the average state space method [7], it is possible to model the aforementioned converter according to the following expression:

$$\dot{x} = Ax + Bu \tag{5}$$

For this purpose, the considered variables are the current through the equivalent inductor and the voltage across capacitor *C*. A linearized model for the power stage valid for the operating point of the converter can then be derived, which also includes the output filter.
There are several techniques available in literature for the control of dc-dc converters [19]. Average current mode control has been chosen in this work, which is represented in Fig. 7 and is based on two independent loops. The first one is responsible for controlling the current through the supercapacitor module, while the second one controls the voltage across the capacitor *C*. A PI (proportional-integral) controller is used in both loops, whose proper design depends on the transfer functions of the converter obtained in the modeling.

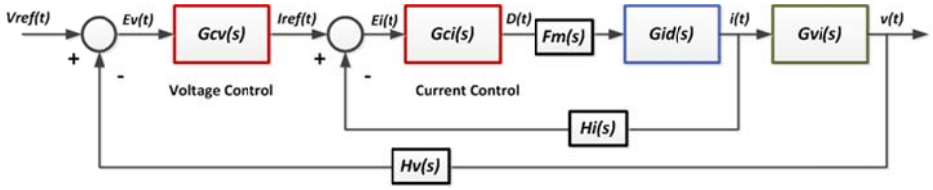

Fig. 7: Block diagram of the control system

The discretization of controllers was performed using the methodology presented in [16] and validated in [5] for the digital implementation of the control system. Therefore, the controllers are designed considering the frequency response of the discrete system by using a similar criterion valid for continuous systems. Fig. 8 represents the simplified discrete controller [5].

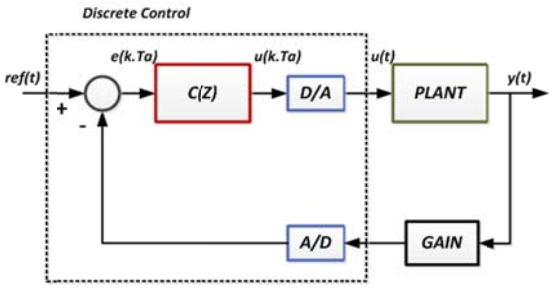

Fig. 8: Simplified block diagram representing the control system in the discrete domain

In order to validate the converter operation, an experimental prototype was developed and assembled in a modular way. The control circuit is implemented in dsPIC30F4011 (Digital Signal Peripheral Interface Controller or Controller, or simply Digital Signal – DSC) from Microchip [14]. Fig. 9 shows a simplified diagram of the complete laboratory setup used in the converter tests. It is possible to verify that PSIM® and MPLAB® are used in the simulation tests. The algorithm executed by the microcontroller is developed in programming language C and compiled using the application software C30. The program also includes fault codes developed in order to protect and ensure the smooth operation of the converter.

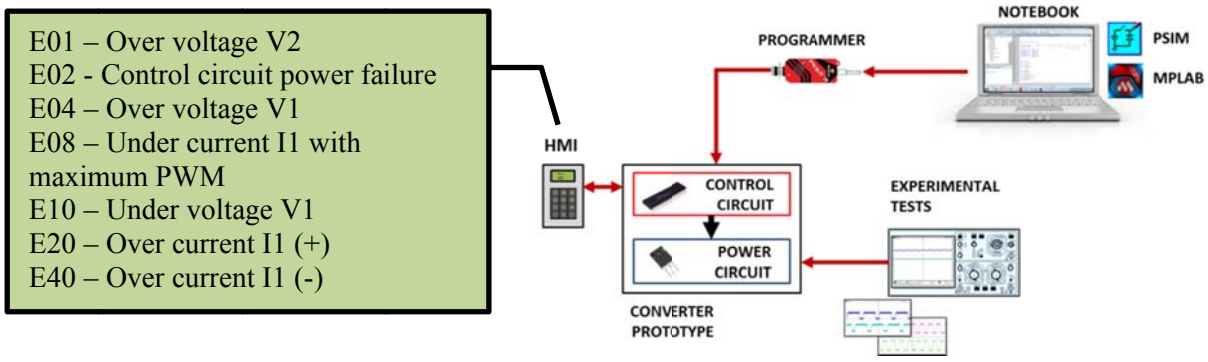

Fig. 9: Representation of the implemented system

Fig. 10 shows the experimental prototype. An HMI (human machine interface) is used to monitor the converter variables (current and voltage) and allow the manual adjustment of some system parameters (duty cycle, protection limits, etc.).

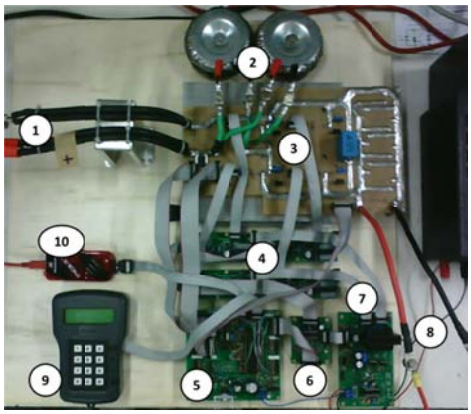

1 - Input voltage (V_1)
2 - Inductors L_1 and L_2
3 - Power circuit
4 – Drivers
5 - Digital Signal Controller (DsPic30f4011)
6 - Serial interface
7 - Power supply
8 - Dc link voltage (V_2)
9 - HMI
10 - Programmer KitPic3

Fig. 10: Experimental prototype of the dc-dc converter

In order to ensure the accurate converter operation, two essential points are initially considered: the drive signals for the switches in each phase must be displaced by 180° and a dead time must exist between the PWM signals applied to complementary switches in a same leg. Fig. 11 shows such conditions, where the phase displacement between the drive signals of the switches does exist. According to the waveforms that represent the currents through the inductors (I_{L1} and L2) and the voltages across the switches (V_{S1} and V_{S2}) in Fig. 12, it is also possible to observe the behavior of the interleaved converter. It is worth to observe that the aforementioned waveforms are obtained under load condition of 1 kW using a dc voltage source V_1=48 V.

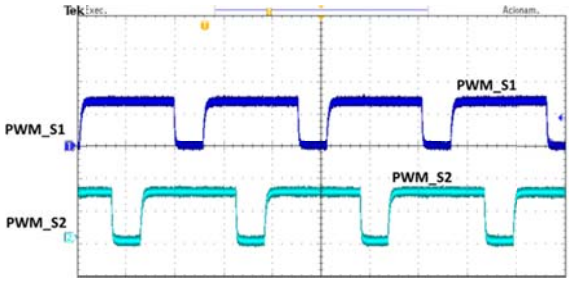

Scales: PWM_S1 and PWM_S2 (10 V/div);
Time (20 µs/div)
(a)

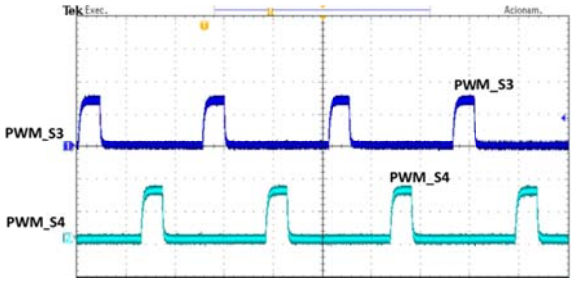

Scales: PWM_S3 and PWM_S4 (10 V/div);
Time (20 µs/div)
(b)

Fig. 11: PWM drive signals of the active switches

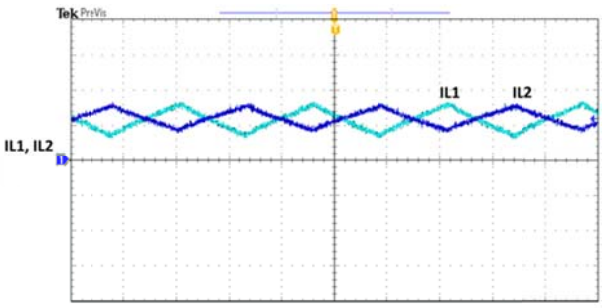

Scales: Currents I_{L1} and I_{L2} (10A/div);
Time (20 µs/div)
(a)

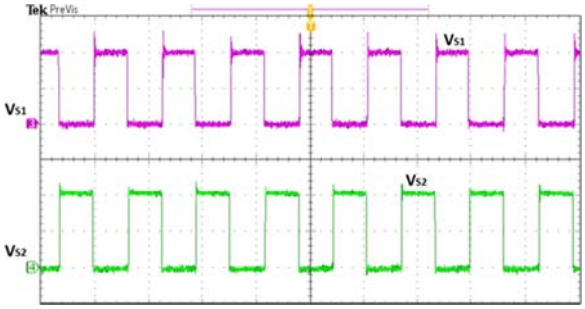

Scales: Voltages V_{S1} and V_{S2} (50 V/div);
Time (40 µs/div)
(b)

Fig. 12: Currents through inductors L_1 and L_2 and voltages across switches S_1 and S_2

Experimental results for the converter in either buck mode or boost mode under closed loop operation are also presented and discussed as follows. The analysis is divided in two stages and depends on the behavior of voltage V_2 and currents I_1 and I_2, which are shown in Fig 13. In the experimental tests, batteries are used to represent both voltage sources V_1 and V_2. In order to evaluate the operation in boost mode, the controller is adjusted so that voltage V_2 remains constant at 98.5 V, which corresponds to the voltage across the dc link. A positive load step from 500 W to 1.5 W is then applied in Fig. 13(a), where it can be seen that the converter is stable. During buck mode operation (Fig. 13(b)), the same aforementioned load is connected to the input side of the converter (corresponding to V_1) and a dc voltage source V_2 represented by a battery is used. The controller is adjusted so that voltage V_2=96 V remains constant. Since the voltage across the battery bank is 98.5 V, which is higher than voltage V_2, power tends to flow in the opposite direction. Initially, the battery bank remains disconnected, as there is no current flowing through the converter. After its connection to the system, it can be seen that currents I_1 and I_2 become negative so that the load at the input side is supplied. When the battery bank is once again disconnected, the current becomes zero. However, it can be seen that voltage V_2 is stable during the load step.

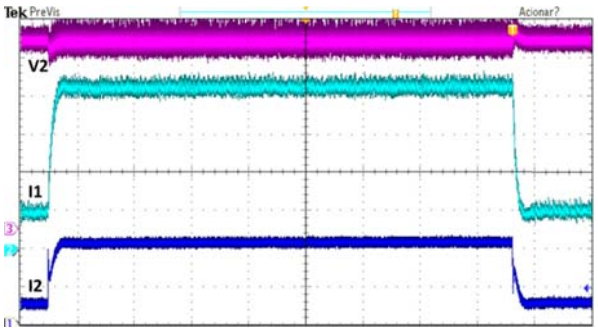

Scales: Voltage V_2 (20 V/div); Currents I_1 and I_2 (10 A/div); Time (100 ms/div)

(a) Boost mode

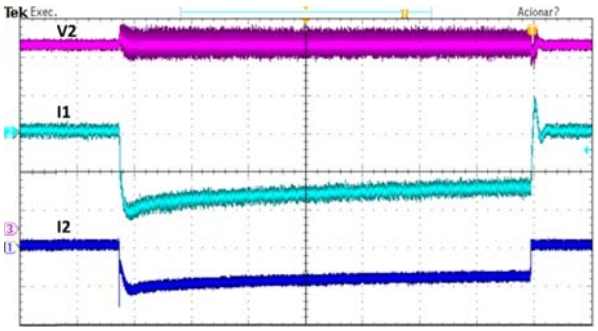

Scales: Voltage V_2 (20 V/div); Currents I_1 and I_2 (10 A/div); Time (100 ms/div)

(b) Buck mode

Fig. 13: Voltage V_2 and currents I_1 and I_2

Conclusion

The use of supercapacitors is somewhat new, which represents a technology in constant progress with increasingly promising results. According to the literature review carried out in this paper, it is possible to notice that supercapacitors have been used as a fast power supply in MGs and EVs. It is then evident that SCs are adequate for numerous applications since there are several commercial approaches for this purpose.

The study has also demonstrated that the bidirectional interleaved boost converter is commonly used in applications involving SCs. The evaluation of the aforementioned converter shows that the input current ripple is reduced significantly and power is equally shared between the two phases, while a simple structure results. A 2-kW prototype has been developed to connect a 165-F/48-V supercapacitor module to a 96-V dc link, as the simulation and experimental results satisfactorily validate the theoretical assumptions.

References

[1] A. A. Ferreira and J. A. Pomílio, “Estado da arte sobre a aplicação de Supercapacitores em Eletrônica de Potência”, Eletrônica de Potência, Vol. 10, nº 2, November 2005.

[2] A. A. Ferreira, J. A. Pomilio, E. P. Silva and D. V. P. Cambra, “Metodologia para dimensionar múltiplas fontes de suprimento de energia de veículos elétricos”. VE 2007 - 5° Seminário e Exposição de Veículos Elétricos. Rio de Janeiro, 2007.

[3] F. Lium, “30 kW Power Boost System for Drive Trains for Electric Vehicles Based on Supercapacitor Technologies”, Master of Science in Energy and Environment. Norwegian University of Science and Technology. Submission in June 2007.

[4] F. S. Garcia, “Conversores CC-CC elevadores de tensão, não isolados, com ganhos estáticos elevados”, dissertação de mestrado, Faculdade de Engenharia Elétrica e Computação, Universidade Estadual de Campinas, 2010.
[5] G. Franklin *et al*. Digital control of dynamic systems. 3. ed. Half Moon Bay: Ellis-Kagle Press, 2006.
[6] H. Martin and J. Martin, “Battery-Supercapacitor Energy Storage”, Master of Science Thesis in Electrical Engineering. Department of Energy and Environment, Division of Electric Power Engineering, Chalmers University of Technology. Göteborg, Sweden, 2008.
[7] J.A. Pomílio. Fontes chaveadas. Apostila da disciplina Fontes Chaveadas, Faculdade de Engenharia Elétrica e de Computação, Universidade Estadual de Campinas. Campinas: FEEC, 2010. Available at <http://www.dsce.fee.unicamp.br/~antenor/fontchav.html>. Accessed on Oct. 01, 2013.
[8] J. Kloetzl and D. Gerling, “An Interleaved Buck-Boost-Converter Combined with a Supercapacitor-Storage for the Stabilization of Automotive Power Nets”, Werner Heisenberg-Weg 39 Neubiberg, Germany, 2011.
[9] J. Zhang, “Bidirectional DC-DC Power Converter Design Optimization, Modeling and Control”, dissertation submitted to the faculty of the Virginia Polytechnic Institute and State University in partial fulfillment of the requirements for the degree of Doctor of Philosophy in Electrical Engineering, Jan. 2008.
[10] LS Ultracapacitor [Online]. Available at <http://www.lsmtron.com>. Accessed on Oct. 13, 2013.
[11] MATHWORKS. Supercapacitor. MathWorks, [2013]. Available at <http://www.mathworks.com/help/physmod/sps/powersys/ref/supercapacitor.html>. Accessed on Nov. 05, 2013.
[12] Maxwell Technologies. Available at <http://www.maxwell.com/ultracapacitors>. Accessed on Aug. 18, 2013.
[13] Maxwell Technologies, “Product Guide – Maxwell Technologies BOOSTCAP Ultracapacitors”, Doc. No. 1014627.1 © 2009 Maxwell Technologies®, Inc [Online]. Available at <http://www.maxwell.com/products/ultracapacitors/docs/1014627_boostcap_product_guide.pdf>. Accessed on Aug. 18, 2013.
[14] Microchip. DsPIC30F4011/4012 data sheet: high performance digital signal controllers. Microchip, 2005. Available at <http://ww1.microchip.com/downloads/en/devicedoc/70135C.pdf >. Accessed on Feb. 18, 2014.
[15] M. Ehsani, Y. Gao, S. E. Gay and A. Emadi, “Modern Electric, Hybrid Electric, and Fuel Cell Vehicles: Fundamentals, Theory, and Design”, Boca Raton, FL: CRC Press, ISBN: 0-8493-3154-4, Dec. 2004.
[16] M. Klepl. Evaluation of digital control law design in the W’-plane. *In*: AMERICAN CONTROL CONFERENCE, 1986, Seattle. Proceedings... Nova York: IEEE, 1986.
[17] M. Moshirvaziri, “Ultracapacitor/Battery Hybrid Energy Storage Systems for Electric Vehicles”, a thesis submitted in conformity with the requirements for the degree of Master of Applied Science Graduate Department of Electrical and Computer Engineering University of Toronto. 2012.
[18] M. S. Halper and J. C. Ellenbogen, “Supercapacitors: A Brief Overview”, MITRE McLean, Virginia, 2006.
[19] M. K. Kazimierczuk, “Pulse-width Modulated DC–DC Power Converters”, Wiley, Ohio, USA, 2008.
[20] Nesscap Ultracapacitors [Online]. Available at <http://www.nesscap.com/product/overview.jsp>. Accessed on Oct 13, 2013.
[21] R. Sathishkumar, S. K. Kollimalla and M. K. Mishra, “Dynamic energy management of micro grids using battery super capacitor combined storage”, published in India Conference (INDICON), 2012 Annual IEEE, pp. 1078–1083.
[22] R. W. Ericson and D. Maksimovic, “Fundamentals of Power Electronics”, second edition, Kluwer Academic Publishers. NJ, USA, 2000.
[23] S. Maniktala, “Switching Power Supplies A to Z”, USA, Newnes, 2006.
[24] S. M. Lukic, J. Cao, R. C. Bansal, F. Rodriguez, and A. Emadi, “Energy Storage Systems for Automotive Applications”. IEEE Transactions on Industrial Electronics, VOL. 55, NO. 6, JUNE 2008.
[25] Vinatech [Online]. Accessed on <http://www.supercapacitorvina.com/product/edlc.html>. Accessed on Oct 13, 2013.
[26] W. Bingbing, Y. Zhongdong, and X. Xiangning, “Super-capacitors energy storage system applied in the microgrid”, published in the 5th IEEE Conference on Industrial Electronics and Applications (ICIEA), 2010, Taichung, pp. 1002-1005.